



TITLE:

# Numerical simulation of solid particle behaviors in fluid flow by using a numerical method coupling technique

AUTHOR(S):

OHTSUKI, Satoshi; MATSUOKA, Toshifumi

---

CITATION:

OHTSUKI, Satoshi ...[et al]. Numerical simulation of solid particle behaviors in fluid flow by using a numerical method coupling technique. International Journal of the JCRM 2009, 4(2): 61-67

ISSUE DATE:

2009-06

URL:

<http://hdl.handle.net/2433/109961>

RIGHT:

Copyright © 2009 Japanese Committee for Rock Mechanics



# International Journal of the JCRM

Japanese Committee for Rock Mechanics

Volume 4, Number 2, June 2009, pp.61-67  
[ISSUE PAPER]

## Numerical simulation of solid particle behaviors in fluid flow by using a numerical method coupling technique

Satoshi OHTSUKI\* & Toshifumi MATSUOKA\*

\* Member of ISRM: Dept. of Civil and Earth Resources Eng., Graduate School of Eng., Kyoto University, Katsura, Nishikyo-ku, Kyoto 615-8540  
Japan

Received 07 10 2008; accepted 02 06 2009

### ABSTRACT

In rock engineering, the behavior of solid particles in a fluid flow has become an important topic. This paper demonstrates the effectiveness of a numerical simulation method based on the micro-mechanics of the fluid-solid interaction that couples the lattice-Boltzmann method (LBM) and the discrete element method (DEM). LBM is known to be a suitable technique for simulating fluid flow in complex and time-varying geometries with boundaries. DEM has attracted much attention among rock engineers as a useful simulation technique for large deformation problems. With the coupling of both methods, the complex motions of solid particles in a fluid flow can be simulated. To verify this, the sedimentation behavior of a single circular particle is simulated in a fluid with different Reynolds numbers, and the results are compared with FEM. In addition, the drafting, kissing, and tumbling (DKT) phenomenon between two particles in a fluid is modeled and reasonable results are obtained. The results of these case studies suggest that the method of coupling LBM and DEM can be an effective technique for simulating many kinds of engineering problems.

*Keywords: Fluid-solid mechanics, lattice-Boltzmann method, discrete element method, settling particle, DKT phenomenon*

### 1. INTRODUCTION

Fluid-solid interaction mechanics has been examined with regard to various problems in the field of rock engineering. Typical problems involve the behavior of solid particles in fluid flow, such as sedimentation, fluidization, and erosion. Working out the mechanics of individual solid particles in fluid flow is essential for understanding the overall these types of problems. Their dynamic behavior is very complicated owing to the complex interactions between individual particles and their interactions with the surrounding gas, liquid, or walls.

The lattice-Boltzmann method (LBM; McNamara and Zanetti 1988, Higuera and Jimenez 1989) has emerged as a powerful alternative tool for solving fluid flows, in addition to conventional finite element and finite volume-based fluid solvers (Feng et al. 2007). This method is suitable for the simulation of fluid flow within complicated and time-varying computational boundary geometries.

In the particle transport problems described above, moving boundary conditions must be considered. Ladd proposed a new boundary condition between the fluid and a moving particle using LBM (Ladd 1994). In the proposed method, however, the evaluated interface force may suffer from severe oscillations when the particle moves across the grid with high velocity. This is caused by the use of a

simplified fluid-solid boundary and interactions. The immersed moving boundary (IMB) method is known as a general modeling technique for the interactions between fluid and solid. Noble and Torczynski incorporated this modeling technique into LBM and achieved more accurate computations (Noble and Torczynski 1998).

In addition, another numerical method is required for the evaluation of solid particle behavior. The discrete element method (DEM; Cundall and Strack 1979) satisfies this requirement for a system of discrete particles. DEM is well known as a useful methodology for discontinuous body analysis; in particular, it has received attention for its application to large deformation problems in rock engineering. In this method, a material is modeled as an assembly of particles that interact with each other. In general, a linear spring-dashpot system is adopted for the normal and tangential forces between particles in contact, and the tangential force is limited by Coulomb friction. At each time step, particles in contact are searched for, their contact forces are calculated, and then their positions are updated by integrating their equations of motion based on Newton's second law.

Based on these considerations, a methodology coupling LBM and DEM was proposed (Cook et al. 2000). This coupled methodology has begun to be applied to fluid-solid systems such as near-wellbore failure phenomena (Cook et al. 2004) and the interaction between two settling particles (Qi

1999, Niu et al. 2006, Strack and Cook 2007).

Moreover, DEM has been coupled with computational fluid dynamics (CFD) to describe particle-fluid flows (Tsuiji et al. 1993, Xu and Yu 1997, Zhu et al. 2008). Some of the advantages of LBM over Navier-Stokes CFD include the potential for using an Eulerian grid and high space-time resolution, as well as efficient and robust implementation in complex fluid domains (Chen et al. 2003). A key advantage of LBM over traditional CFD (Tezduyar 2001) is its ability to be efficiently and robustly coupled to a large number of discrete elements. The main computational obstacle in the Lagrangian CFD approach is the generation of a valid mesh for dense particle flows where the sustained contact of discrete elements is a dominant physical phenomenon (Leonardi et al. 2008). From this point of view, the coupled LBM and DEM methodology is probably a more promising approach.

In this paper, we attempt to simulate the sedimentation behavior of circular particles in a fluid flow using the methodology of coupled LBM and DEM. We show the results of a numerical simulation of single circular particles settling in a fluid acted upon by the gravitational force. We qualitatively validate this simulation method by comparing the results to a finite element model. In addition, we reproduce the drafting, kissing, and tumbling (DKT) phenomenon between two particles, and examine its detailed mechanism. In particular, we examine the relationship between the position of two particles and the magnitude of the hydrodynamic force exerted on them.

## 2. NUMERICAL SIMULATION METHODS

### 2.1 Lattice-Boltzmann method

In recent years, the lattice-Boltzmann method (LBM) has made brilliant progress as a new technique in numerical fluid dynamics. This technique is different from conventional numerical fluid dynamics, which uses discrete Navier-Stokes equations. In this regard, the technique defines the distribution functions of “virtual fluid particles” and solves the evolution equation of the distribution functions. The technique does not incorporate Navier-Stokes equations, but it has been demonstrated theoretically that the calculation results are the same as those from Navier-Stokes equations.

The computational domain is spatially-discretized by the lattice, and an extremely regular model is used for the motion of the particles in LBM. Concurrently, it is necessary to apply an appropriate collision term satisfying the conservation law of the flow. Many simulation models using various collision terms and velocity models have been suggested. In this work, a 2D incompressible fluid flow with density  $\rho$  and kinematic viscosity  $\nu$  is simulated in a computational domain that is divided into a regular lattice with spacing  $h$  in both the  $x$  and  $y$  directions. The Bhatnagar-Gross-Krook (BGK) model and the D2Q9 model (Figure 1) is used for the collision term and the velocity model, respectively (Qian et al. 1992, Succi et al. 1993). In this discretization scheme, the fluid at each node moves to its eight neighboring nodes at different velocities  $\mathbf{e}_i (i=1, \dots, 8)$  or rests with zero velocity  $\mathbf{e}_0$ .

The evolution of the density distribution functions at each time step is formulated as follows:

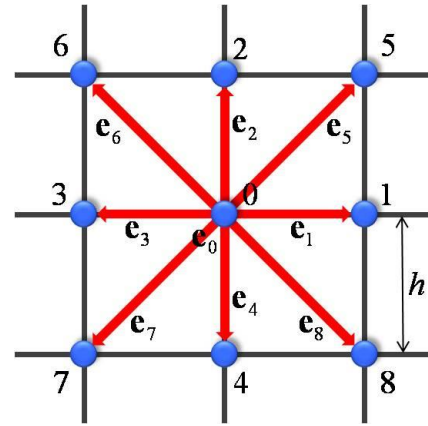


Figure 1. The D2Q9 model.

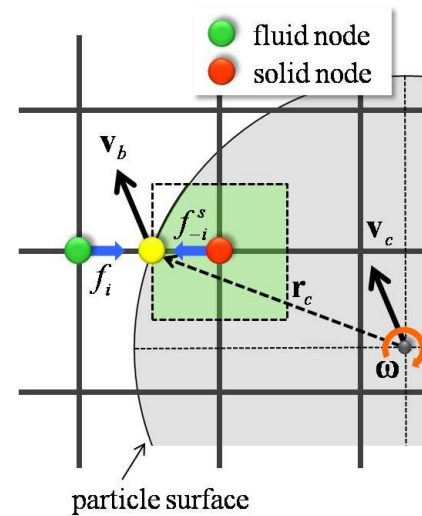


Figure 2. Noble and Torczynski's scheme.

$$f_i(\mathbf{x} + \mathbf{e}_i \Delta t, t + \Delta t) = f_i(\mathbf{x}, t) - \frac{1}{\tau} [f_i(\mathbf{x}, t) - f_i^{eq}(\mathbf{x}, t)] \quad (1)$$

where  $f_i (i=0, \dots, 8)$  are nine fluid density distribution functions for any node  $\mathbf{x}$ ,  $\mathbf{x} + \mathbf{e}_i \Delta t$ ;  $\tau$  is the relaxation time; and  $f_i^{eq}$  are the equilibrium distribution functions defined as

$$f_0^{eq} = w_0 \rho \left( 1 - \frac{3}{2C^2} \mathbf{v} \cdot \mathbf{v} \right) \quad (2a)$$

$$f_i^{eq} = w_i \rho \left( 1 + \frac{3}{C^2} \mathbf{e}_i \cdot \mathbf{v} + \frac{9}{2C^4} (\mathbf{e}_i \cdot \mathbf{v})^2 - \frac{3}{2C^2} \mathbf{v} \cdot \mathbf{v} \right), (i=1, \dots, 8) \quad (2b)$$

Here,  $w_i$  are the weighting functions, and  $C$  is the lattice speed with lattice spacing  $h$  and discrete time step  $\Delta t$ :

$$w_0 = \frac{4}{9}, w_{1,2,3,4} = \frac{1}{9}, w_{5,6,7,8} = \frac{1}{36} \quad (3)$$

$$C = \frac{h}{\Delta t} \quad (4)$$

The relaxation time  $\tau$  shows a non-dimensional time scale that the density distribution function at each node takes to approach the equilibrium distribution functions. The macroscopic fluid parameters, density  $\rho$  and velocity  $\mathbf{v}$ , at each node can be recovered as follows:

$$\rho = \sum_{i=0}^8 f_i, \rho \mathbf{v} = \sum_{i=0}^8 f_i \mathbf{e}_i \quad (5)$$

The kinematic viscosity coefficient of the fluid  $\nu$  can be determined as follows (He and Luo 1997):

$$\nu = \frac{1}{3} \left( \tau - \frac{1}{2} \right) \frac{h^2}{\Delta t} \quad (6)$$

There are three parameters for the fluid viscosity as shown by Equation (6): the relaxation time  $\tau$ , the lattice spacing  $h$ , and the discrete time step  $\Delta t$ . This equation indicates that these three parameters cannot be selected independently, but have to be related to achieve a desired fluid viscosity (Feng et al. 2007).

The standard formulation of LBM was developed for laminar flows at low Reynolds numbers (typically around 100 or less). In this study, the coupled methodology uses standard LBM. Many engineering problems nevertheless exhibit turbulent behavior. Recently, new attempts have been made to incorporate some existing turbulence models such as large eddy simulation into LBM (Feng et al. 2007).

## 2.2 Moving solid boundary condition

A moving boundary condition is essential for the coupled LBM and DEM methodology. Many moving boundary conditions for LBM have been proposed. In this study, we adopt a scheme proposed by Noble and Torczynski (Noble and Torczynski 1998, Han et al. 2007, Feng et al. 2007). In this scheme, the collision operator in the LBM equation is modified by the solid area fraction  $\gamma$  in each nodal cell (Figure 2). Thus, Equation (1) for the nodes covered by the solid particle becomes

$$f_i(\mathbf{x} + \mathbf{e}_i \Delta t, t + \Delta t) = f_i(\mathbf{x}, t) - \frac{1}{\tau} (1 - \beta) [f_i(\mathbf{x}, t) - f_i^{eq}(\mathbf{x}, t)] + \beta f_i^m \quad (7)$$

where  $\beta$  is a weighting function that depends on the solid area fraction  $\gamma$  in each nodal cell:

$$\beta = \frac{\gamma(\tau - 0.5)}{(1 - \gamma) + (\tau - 0.5)} \quad (8)$$

$f_i^m$  is a new collision term that accounts for the bounce-back of the non-equilibrium part of the distribution function and is given by

$$f_i^m = f_{-i}(\mathbf{x}, t) - f_i(\mathbf{x}, t) + f_i^{eq}(\rho, \mathbf{v}_b) - f_{-i}^{eq}(\rho, \mathbf{v}) \quad (9)$$

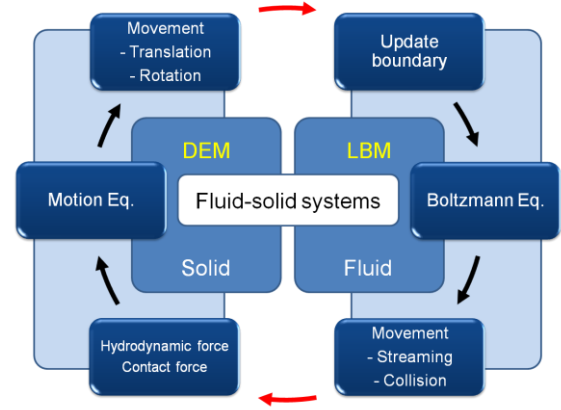


Figure 3. The cycle of computation for coupled LBM and DEM.

where  $-\mathbf{i}$  denotes the direction opposite of  $\mathbf{i}$ .

The hydrodynamic forces and torque exerted on a particle can be computed as

$$\mathbf{F}_{fluid} = \frac{h^2}{\Delta t} \left[ \sum_n \left( \beta_n \sum_i f_i^m \mathbf{e}_i \right) \right] \quad (10)$$

$$\mathbf{T}_{fluid} = \frac{h^2}{\Delta t} \left[ \sum_n (\mathbf{x}_n - \mathbf{x}_c) \times \sum_n \left( \beta_n \sum_i f_i^m \mathbf{e}_i \right) \right] \quad (11)$$

where  $n$  is the number of nodes covered by a particle.

## 2.3 Discrete element method

The discrete element method (DEM) is one of the simulation methods suitable for discontinuous bodies such as rock mass and ground. This method can simulate the dynamic behavior of rock mass by considering the simulation object as an aggregate of rigid particles. Interparticle force is generated by setting a virtual spring. The equations of motion for each particle are solved to track its behavior.

The equations of motion for solid particles in a fluid are as follows:

$$m\mathbf{a} + c\mathbf{v} = \mathbf{F}_{solid} + \mathbf{F}_{fluid} \quad (12)$$

$$I\ddot{\boldsymbol{\theta}} = \mathbf{T}_{solid} + \mathbf{T}_{fluid} \quad (13)$$

where  $m$  is the particle mass;  $\mathbf{a}$  and  $\mathbf{v}$  the particle acceleration and velocity, respectively;  $c$  the damping coefficient;  $I$  moment of inertia; and  $\ddot{\boldsymbol{\theta}}$  the angular acceleration.

## 2.4 Outline of fluid-solid systems

The cycle of computation for the coupled LBM and DEM methodology is as follows (Figure 3):

(1) Fluid motion is simulated by solving the Boltzmann equation.

(2) The hydrodynamic force exerted on each particle is calculated.

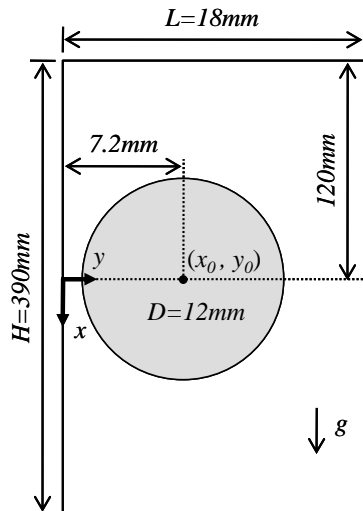


Figure 4. Model for the simulation of a settling circular particle.

Table 1. Input parameters for the simulation of a settling circular particle.

DEM	Discrete time step	$5.0 \times 10^{-6}$ [sec]
	Solid density	$2.0 \times 10^3$ [kg/m <sup>3</sup> ]
	Particle radius	$6.0 \times 10^{-3}$ [m]
LBM	Discrete time step	$3.6 \times 10^{-5}$ [sec]
	Fluid density	$1.0 \times 10^3$ [kg/m <sup>3</sup> ]
	Number of nodes	$652 \times 32$ [-]
	Lattice spacing	$6.0 \times 10^{-4}$ [m]
	Gravitational acceleration	9.8 [m/sec <sup>2</sup> ]
	Simulation duration	$1.8 \times 10^1$ [sec]

Table 2. The relaxation times and kinematic viscosity coefficients.

	Relaxation time $\tau$ [-]	Kinematic viscosity coefficient $\nu$ [m <sup>2</sup> /sec]
Case 1	0.555	$1.83 \times 10^{-4}$
Case 2	0.528	$9.33 \times 10^{-5}$
Case 3	0.519	$6.33 \times 10^{-5}$

(3) The hydrodynamic and contact forces between particles are regarded as external forces. The translational and rotational motions of each particle are calculated by solving the motion equation.

(4) A new boundary for the fluid is formed by updating the particle position.

### 3. SIMULATION OF A SETTLING CIRCULAR PARTICLE

#### 3.1 Settling of a single circular particle

To evaluate the newly developed program, we carried out a numerical simulation of the sedimentation behavior of a single circular particle in a fluid. The settling of a circular particle in a vertical channel between parallel walls was computed by Feng et al. (1994) using the finite element method (FEM). In their numerical experiment, a circular particle was released with zero initial velocity, and set at an

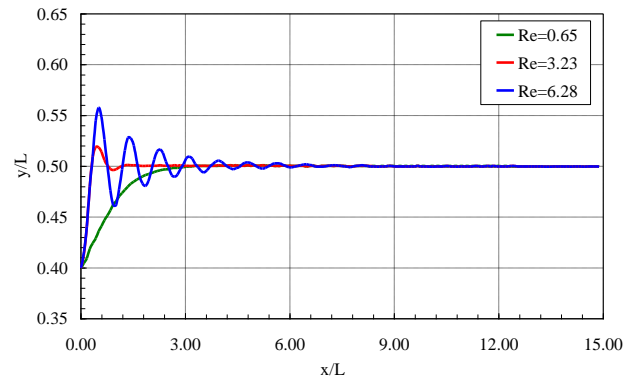


Figure 5. Settling particle trajectories computed by FEM.

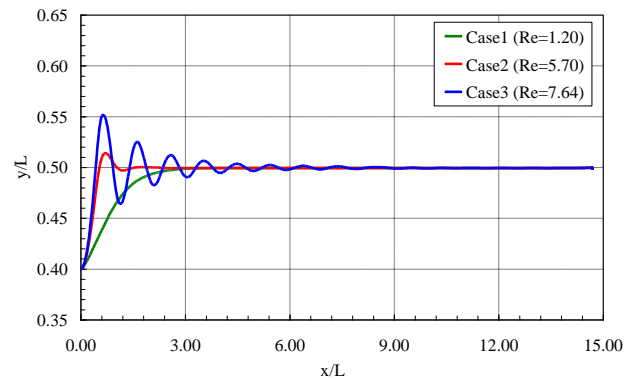


Figure 6. Settling particle trajectories in this study.

initial offset from the center of the channel. They discovered several different modes of sedimentation for a circular particle associated with Reynolds numbers of different magnitudes. We compared our computational results with the results from Feng et al. (1994) for each Reynolds number. In our simulation, the Reynolds number is based on the maximum flow velocity and the particle diameter.

#### 3.2 Simulation condition

Figure 4 describes the initial state of the simulation model. The x-axis is located vertically down on the left wall and the y-axis is located horizontally to the right. The computational domain is 18 mm wide (L) by 390 mm height (H). The circular particle is 12 mm in diameter (D). The initial central coordinate of this circular particle is  $(x_0, y_0) = (0, 0.4L)$ . The particle/fluid density ratio is 2.0.

The input parameters are given in Table 1. The relaxation time  $\tau$  is one of the parameters that determine the fluid viscosity, and by varying its value we obtain different values of the kinematic viscosity coefficient of the fluid (Equation (6)). Table 2 lists the values of the relaxation time used in this simulation and the resulting values of the kinematic viscosity coefficient. It can be seen that the viscosity of the fluid used in this simulation is rather high compared to water.

#### 3.3 Settling particle trajectories

By comparing the results of the numerical experiments by Feng et al. (1994) (Figure 5) to the results of our simulation using the parameters listed in Tables 1 and 2 (Figure 6), it can be seen that the settling particle trajectories related to each

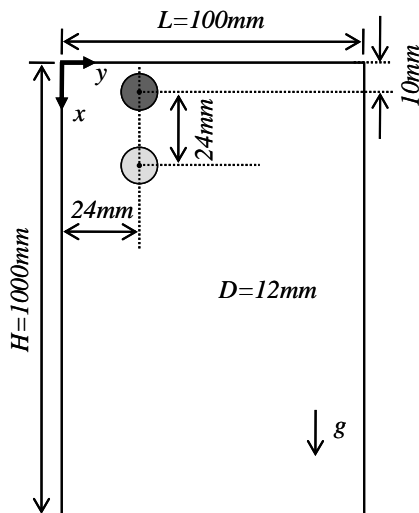


Figure 7. Model for simulating the DKT phenomenon.

Table 3. Input parameters for the DKT phenomenon simulation.

DEM	Discrete time step	$5.0 \times 10^{-6}$	[sec]
	Solid density	$2.5 \times 10^3$	[kg/m <sup>3</sup> ]
	Particle radius	$6.0 \times 10^{-3}$	[m]
	Friction coefficient between particles	0.25	[-]
	Spring stiffness (normal)	$2.5 \times 10^6$	[N/m]
	Spring stiffness (tangential)	$1.0 \times 10^6$	[N/m]
	Damping coefficient	1.0	[Nsec/m]
LBM	Discrete time step	$1.0 \times 10^{-4}$	[sec]
	Fluid density	$1.0 \times 10^3$	[kg/m <sup>3</sup> ]
	Number of nodes	1002	[-]
	Lattice spacing	$1.0 \times 10^{-3}$	[m]
	Relaxation time	0.65	[-]
	Gravitational acceleration	9.8	[m/sec <sup>2</sup> ]
	Simulation duration	5.0	[sec]

Reynolds number seem to follow a similar tendency. For a low Reynolds number, the particle drifts toward the center, either monotonically approaching it or overshooting it with a damped oscillation. In the case of a higher Reynolds number, the particle settles after oscillating regularly or irregularly around the center.

Decreasing the value of the relaxation time (or increasing the Reynolds number) increases the amplitude of these trajectories. This seems to be caused by the low drag force exerted on the particle. Moreover, it is possible that the different definition of Reynolds numbers and the oversized lattice spacing are the reasons that the two results are different.

#### 4. DKT PHENOMENON SIMULATION

##### 4.1 DKT phenomenon

The drafting, kissing, and tumbling (DKT) cycle was

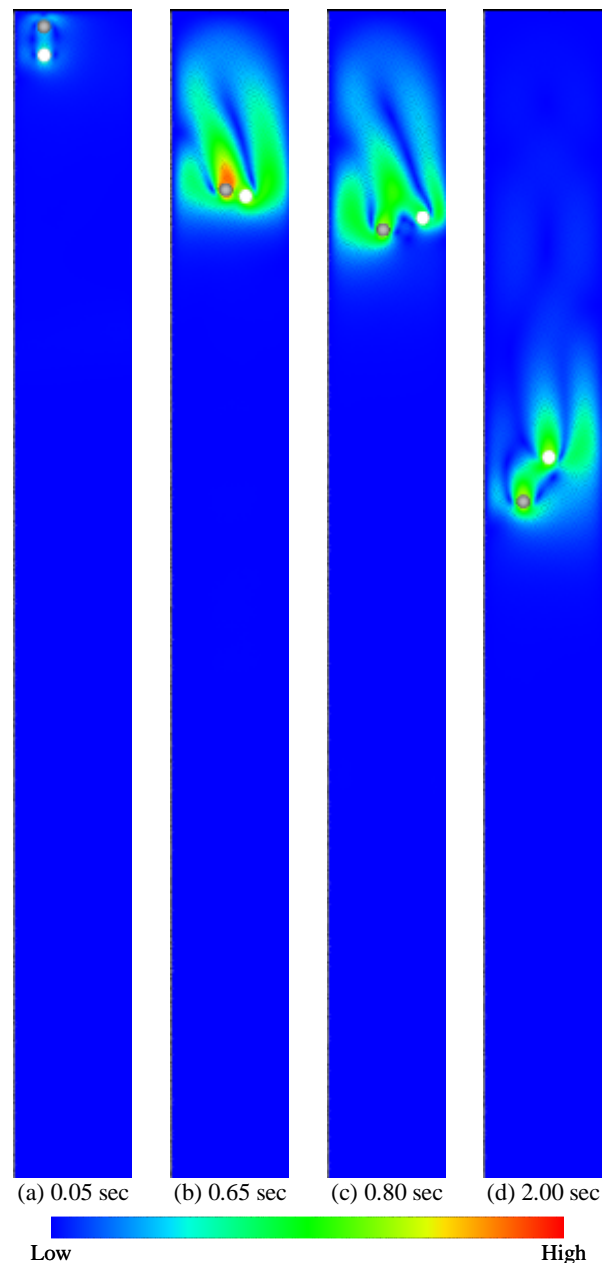


Figure 8. The first DKT cycle.

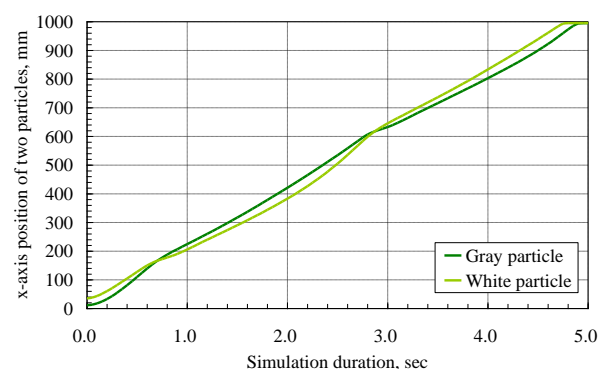


Figure 9. The x-axis position of two circular particles vs. simulation duration.



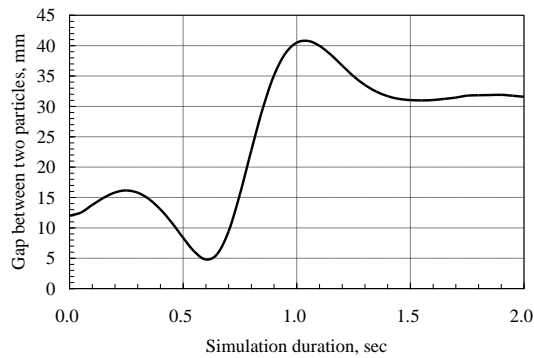


Figure 10. The gap between two circular particles.

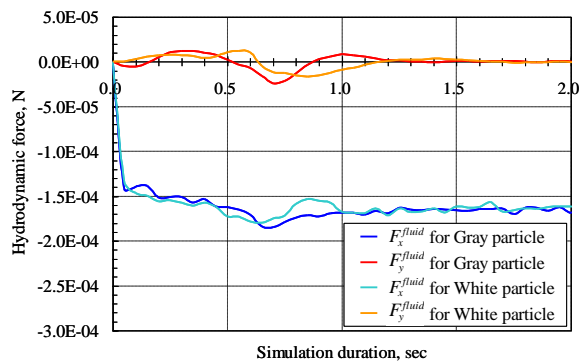


Figure 11. The hydrodynamic forces exerted on two circular particles.

discovered by experiment (Fortes et al. 1987). This phenomenon occurs between particles settling in a fluid. The phenomenon consists of the following three stages. In the drafting stage, the upper particle is accelerated by the low-pressure wake of the lower particle. In the kissing stage, the upper particle overtakes and possibly contacts the lower particle. In the tumbling stage, they tumble with the upper particle assuming the lower one.

#### 4.2 Sedimentation behavior of two circular particles

We simulated the sedimentation behavior of two circular particles by using this coupled LBM and DEM methodology. Figure 7 shows the initial state of the simulation model. The computational domain is 100 mm wide (L) by 1000 mm height (H). The two circular particles are 12 mm in diameter. The upper particle is gray, and the lower particle is white. The particle/fluid density ratio is 2.5 and the input parameters are given in Table 3.

In the first DKT cycle ( $Re = 1.87$ ) obtained by this simulation (Figure 8), the gray particle is first accelerated by the high velocity field behind the white particle. Next, the gray particle catches up with the white particle and the two particles replace each other. In this simulation, the DKT cycle occurred twice (Figure 9).

The gap between the two settling particles is shown in Figure 10. In the first DKT cycle, the minimum gap is 4.77 mm at  $t = 0.61$  sec. Figures 11 and 12 show the x and y components of the hydrodynamic forces exerted on the two particles and the settling velocities of the particles, respectively. The upward force exerted on the two particles as the drag force in the fluid is shown in Figure 11. From 0.0 to

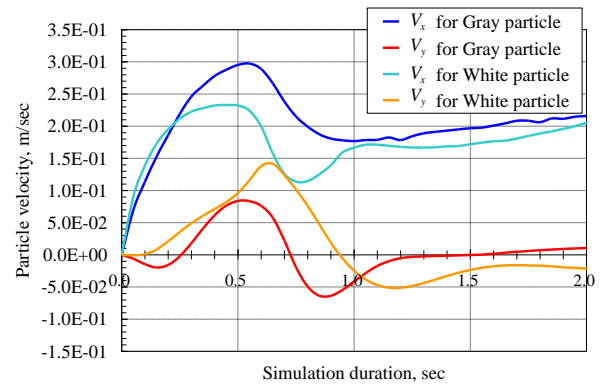


Figure 12. The velocities of the two circular particles.

0.62 sec, the drag force on the white particle is often larger than that on the gray particle. Accordingly, the gray particle has the larger velocity and overtakes the white particle (Figures 10 and 12).

### 5. CONCLUSION

We simulated the sedimentation behavior of a single circular particle and the DKT phenomenon between two circular particles by using a simulator with a model that couples LBM and DEM. In the simulation of single-particle sedimentation, different modes of sedimentation related to Reynolds numbers appeared, and the results agreed well with FEM. In addition, we simulated two sets of the DKT cycle. The most significant finding is that the larger drag force working on the particle in the lower position causes the drafting stage. However, no contact between the two particles occurred in our simulation cases; hence, the conditions for contact occurrence are still unknown.

In the future, we will apply this method to the multi-particle problem of simulating the behavior of sand grains in fluids such as oil production with sand from an unconsolidated formation. Such cases require a very densely packed DEM model, so flow paths between the particles must be modeled rigorously. Another matter to be solved is the relation between the fluid path scale and lattice spacing in the LBM model.

### REFERENCES

- Chen, H., Kandasamy, S., Orszag, S., Shock, R., Succi, S., and Yakhot, V., 2003. Extended Boltzmann kinetic equation for turbulent flows, *Science*, **301**, No.5633, pp.633-636.
- Cook, B., Noble, D., Preece, D., and Williams, J., 2000. Direct simulation of particle-laden fluids, Pacific Rocks 2000, Girard, Lieberman, Breeds, and Doe, eds., Balkema, Rotterdam, The Netherlands, pp.279-286.
- Cook, B. K., Lee, M. Y., DiGiovanni, A. A., Bronowski, D. R., Perkins, E. D., and Williams, J. R., 2004. Discrete element modeling applied to laboratory simulation of near-wellbore mechanics, *International Journal of Geomechanics*, **4** (1), pp.19-27.
- Cundall, P. A., and Strack, O. D. L., 1979. A discrete numerical model for granular assemblies, *Geotechnique*, **29** (1), pp.47-65.
- Feng, J., Hu, H. H., and Joseph, D. D., 1994. Direct simulation of initial value problems for the motion of solid bodies in a Newtonian fluid Part 1. Sedimentation, *Journal of Fluid Mechanics*, **261**, pp.95-134.
- Feng, Y. T., Han, K., and Owen, D. R. J., 2007. Coupled lattice

- Boltzmann method and discrete element modelling of particle transport in turbulent fluid flows: Computational issues, *International Journal for Numerical Methods in Engineering*, **72**, pp.1111-1134.
- Fortes, A. F., Joseph, D. D., and Lundgren, T. S., 1987. Nonlinear mechanics of fluidization of beds of spherical particles, *Journal of Fluid Mechanics*, **177**, pp.467-483.
- Han, K., Feng, Y. T., and Owen, D. R. J., 2007. Coupled lattice Boltzmann and discrete element modelling of fluid-particle interaction problems, *Computers and Structures*, **85**, pp.1080-1088.
- He, X., and Luo, L.S., 1997. Lattice Boltzmann Model for the Incompressible Navier-Stokes Equation, *Journal of Statistical Physics*, **88**, 3/4, pp.927-944.
- Higuera, F., and Jimenez, J., 1989. Boltzmann approach to lattice gas simulations, *Europhys. Lett.* **9**, pp.663-668.
- Ladd, A., 1994. Numerical simulations of fluid particulate suspensions via a discretized Boltzmann-equation. (Parts 1 & 2 ) *Journal of Fluid Mechanics*, **271**, pp.285-339.
- Leonardi, C. R., Owen, D. R. J., and Feng, Y., 2008. Simulation of fines migration using a coupled non-newtonian lattice Boltzmann model and discrete element method, 8th World Congress on Computational Mechanics (WCCM8) & 5th European Congress on Computational Methods in Applied Sciences and Engineering (ECCOMAS 2008), abstract.
- McNamara, G., and Zanetti, G., 1988. Use of the Boltzmann equation to simulate lattice-gas automata, *Phys. Rev. Lett.* **61**, pp.2332-2335.
- Niu, X. D., Shu, C., Chew, Y. T., and Peng, Y., 2006. A momentum exchange-based immersed boundary-lattice Boltzmann method for simulating incompressible viscous flows, *Phys. Lett. A*, **354**, (3), pp.173-182.
- Noble, D., and Torczynski, J., 1998. A lattice Boltzmann method for partially saturated computational cells, *International Journal of Modern Physics C*, **9**, pp.1189-1201.
- Qian, Y. H., d'Humieres, D., and Lallemand, P., 1992. Lattice BGK Models for Navier-Stokes Equation, *Europhys. Lett.*, **17** (6), pp.479-484.
- Qi, D., 1999. Lattice-Boltzmann simulations of particles in non-zero-Reynolds-number flows, *Journal of Fluid Mechanics*, **385**, pp.41-62.
- Strack, O. E. and Cook, B. K., 2007. Three-dimensional immersed boundary conditions for moving solids in the lattice-Boltzmann method, *International Journal for Numerical Methods in Fluids*, **55**, pp.103-125.
- Succi, S., d'Humieres, D., Qian, Y., and Orszag, S. A., 1993. On the small-scale dynamical behavior of lattice BGK and lattice Boltzmann schemes, *Journal of Scientific Computing*, **8**, pp.219-230.
- Tezduyar, T. E., 2001. Finite element methods for flow problems with moving boundaries and interfaces, *Archives of Computational Methods in Engineering*, **8**, pp.83-130.
- Tsuji, Y., Kawaguchi, T., and Tanaka, T., 1993. *Discrete particle simulation of two-dimensional fluidized bed*, *Powder Technology*, **77**, pp.79-87.
- Xu, B. H., and Yu, A. B., 1997. Numerical simulation of the gas-solid flow in a fluidized bed by combining discrete particle method with computational fluid dynamics, *Chemical Engineering Science*, **52**, pp.2785-2809.
- Zhu, H. P., Zhou, Z. Y., Yang, R. Y., and Yu, A. B., 2008. Discrete particle simulation of particulate systems: A review of major applications and findings, *Chemical Engineering Science*, **63**, pp.5728-5770.